

Bright and Color-Saturated Emission from Blue Light-Emitting Diodes Based on Solution-Processed Colloidal Nanocrystal Quantum Dots

Zhanao Tan, Fan Zhang, Ting Zhu, and Jian Xu*

*Department of Engineering Science and Mechanics, Penn State University,
University Park, Pennsylvania 16802*

Andrew Y. Wang,* John D. Dixon, and Linsong Li

Ocean NanoTech LLC., Fayetteville, Arkansas 72702-2168

Qi Zhang and Suzanne E. Mohny

*Material Science and Engineering Department, Penn State University,
University Park, Pennsylvania 16802*

Jerzy Ruzyllo

*Department of Electrical Engineering, Penn State University,
University Park, Pennsylvania 16802*

Received September 14, 2007; Revised Manuscript Received October 23, 2007

ABSTRACT

We report a multilayer solution-processed blue light-emitting diode based on colloidal core/shell CdS/ZnS nanocrystal quantum dots (QDs). At a low-operating voltage of 5.5 V, the device emits spectrally pure blue radiation at 460 nm with a narrow full-width-at-half-maximum bandwidth of 20 nm and high brightness up to 1600 cd/m². Broad-band, long-wavelength emission from the polymer components and deep traps in the QDs are minimized to less than 5% of the total emission.

Recent studies on the electroluminescence (EL) behavior of colloidal nanocrystal quantum dots (QDs) of II–VI compounds have suggested that quantum dot light-emitting diodes (QD-LEDs) could provide a cost-effective alternative to the forthcoming challenges of maximizing efficiency, brightness, color saturation, area, and flexible substrate compatibility for the next generation of flat-panel displays and solid-state lighting.^{1–9} In particular, because of the extremely narrow emission band of monodisperse nanocrystal QD populations (full width at half-maximum (fwhm) \sim 18–30 nm), QD-LEDs have been reported to produce color-saturated red and green emissions of much higher spectral purities than those of liquid crystal displays and organic light-emitting diodes and even 30% greater than bulky cathode ray tubes that are still favored for their excellent color rendition.^{4,6,8,9,10,11,12} Because the display system creates a variety of colors by

varying the relative intensities of the red–green–blue (RGB) subpixels in each screen pixel cell, the enhanced color purity of RGB QD-LEDs will result in an unprecedented improvement in the number of colors that can be displayed. However, such a prospect is dimmed by the slow development to date of bright, color-saturated blue QD-LEDs.¹³

It is well established that the brightness of a display screen is determined by the photometric brightness of the constituent LEDs, which is defined as the wavelength-weighted power emitted by a light source of unit surface area in a particular direction (per unit solid angle), based on the luminous efficacy of human vision¹⁴

$$L_v = 683\bar{y}(\lambda)/S \quad (1)$$

where L_v is the luminance in Cd/m², I is the radiant power in W/sr, S is the surface area of the LED, and $\bar{y}(\lambda)$ is the luminous efficacy, specifying the average sensitivity of the

* Corresponding authors. E-mail: (J.X.) jianxu@engr.psu.edu; (A.Y.W.) awang@oceannanotech.com.

human eye to light of different wavelengths. The blue component (440–490 nm) of the visual spectrum is characterized with low luminous efficacies, unlike its green and red neighbors, ranging from 0.02 to 0.20, as compared to ~ 0.80 – 1.00 for green (520–555 nm) light and ~ 0.20 – 0.70 for orange/red (590–640 nm) light. Therefore, a blue QD-LED demands a higher radiant power, I , than green and orange/red QD-LEDs of the same brightness to compensate for the low-luminous efficacy. Other than brightness, the low efficacy of blue emission also entails critical demands for narrow emission bandwidth and “clean” spectral line shapes of the QD-LED output to achieve the desired blue-saturation.

To date only a few blue QD-LEDs with maximum brightness of $\sim 125 \text{ cd/m}^2$ and fwhm bandwidth $\geq 32 \text{ nm}$ have been demonstrated.^{13,15,16,17} Despite “blue” peak wavelengths (440–478 nm) reported for those QD-LEDs, their emission spectra inevitably exhibited significant tails extending into the green and red region of the spectrum, the integrated intensities of which often contain $\geq 50\%$ of the overall LED radiance power. It is believed that the long-wavelength tails accompanying the blue emission arise from the deep trap emission of nanocrystals as well as the incomplete energy transfer between QDs and the organic molecules comprising the active region of QD-LEDs.^{13,15,16} Because the luminous efficacy of blue light is much lower than that of green light, a broadband, long-wavelength tail beyond the blue portion of the emission could make major contributions to the LED brightness, making the blue emission of QD-LED far from being saturated. The calculation using eq 1 has shown that a “green” tail constituting only 20% of the total emission power will simply double the overall brightness of a blue QD-LED by adding an equal amount of green luminance to the desired blue output.

In this paper, we report on the design and processing of QD-LEDs whose brightness and blue purity far exceed the values reported earlier. The LED in this experiment was configured with a multiple layer structure employing structurally engineered core/shell CdS/ZnS QDs in the emissive region. At a low operation voltage of 5.5V, the device emitted spectrally pure blue with a strikingly narrow fwhm bandwidth of 20 nm and a high brightness up to 1600 cd/m^2 . The long-wavelength tail of the LED output was minimized to less than 5% of the total emission, leading to the highly saturated blue emission from QD-LEDs. The result of our blue-LED study represents a significant improvement over the performance of existing blue QD-LEDs and marks a further step toward the practical application of QD-LED technology in full-color display and solid-state lighting.

The core/shell CdS/ZnS QDs employed in our blue-LED devices were synthesized with an approach modified from that originally proposed by Prot  re et al.¹⁸ The oleylamine/octadecene mixture was used to provide the solvent environment for the nucleation and growth of CdS crystalline cores from cadmium oxide and sulfur precursors at elevated temperatures (250–300  C). The interaction between amine molecules and Cd^{2+} ions in the reaction was found to have a profound impact on the core growth dynamics and led to the substantially narrowed emission bandwidth when the

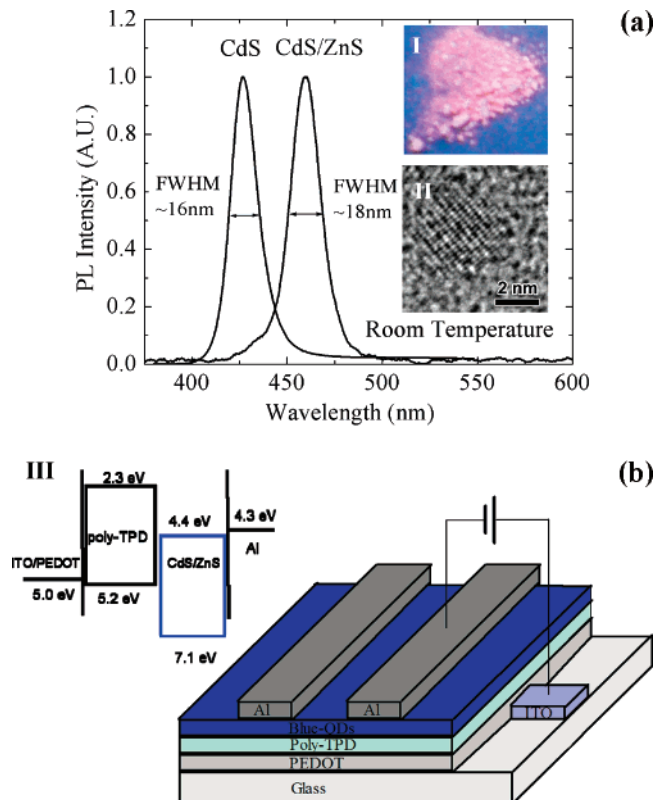


Figure 1. (a) Photoluminescence spectra of CdS cores and core/shell CdS/ZnS nanocrystal QDs stored in tetrachloroethylene solvent. (b) Schematic of the device configuration of the blue QD-LED. Inset I: fluorescent image of QD power under UV light. Inset II: HR-TEM image of a core/shell CdS/ZnS nanocrystal QD. Inset III: simplified energy diagram of the QD-LED device. The energy band structure of QDs is approximated by that of the light-emitting CdS cores.

amine dose was properly controlled.¹⁹ The photoluminescence (PL) emission of CdS cores was tuned to a peak at 420 nm, and the fwhm bandwidth is only 16 nm, as shown in Figure 1a. Upon the shell growth, the monomolecular precursor of zinc ethylxanthate ($\text{Zn}(\text{ex})_2$) was used for its reduced decomposition temperatures (140–150  C), allowing for a sufficiently low shell-synthesis temperature (~ 200  C) to avoid any ripening of the core nanocrystals that could lead to the spectral broadening of the emission peak of the core/shell structures.¹⁸ Such a shell-synthetic strategy was employed in the present study to overcoat CdS cores with three monolayers (MLs) of ZnS shells and to red shift the emission peak to 460 nm while retaining the narrow fwhm bandwidth ($\sim 18 \text{ nm}$) for the emission of core/shell CdS/ZnS QDs (Figure 1a). For their use in the QD-LEDs, the as-prepared core/shell CdS/ZnS QDs were subjected to a multistep precipitation/redissolution process of purification and subsequently dried into solid powders. An important observation in our study was that the involvement of any free ligands in QD powder often introduced impurities and cracklike/pinhole defects to the later spin-coated QD films, leading to low yield and reduced efficiency in the fabricated LEDs.²⁰ The number of repeated purification steps therefore had to be optimized to lower the free ligand concentration in QD samples and at the same time to avoid the significant

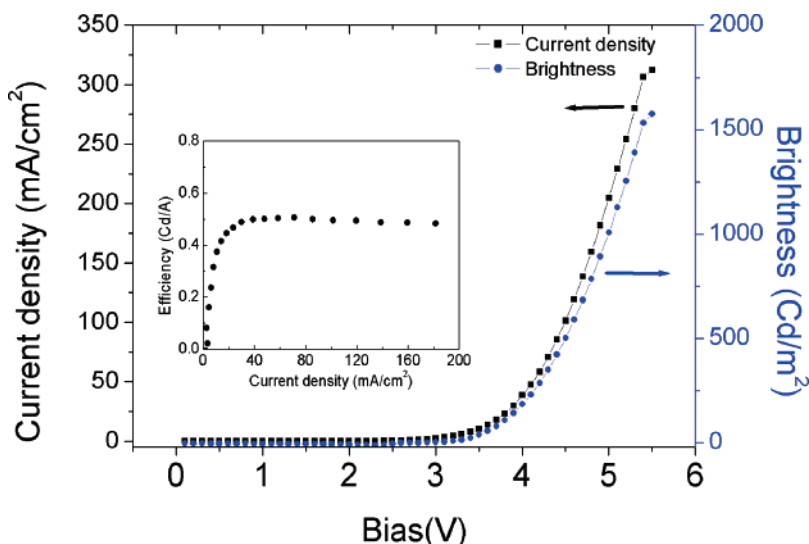


Figure 2. Measured current density and luminance of a blue QD-LED as functions of the applied voltage ($I-V$ and $P-V$). The inset plots the LED luminance efficiency vs the injection current density.

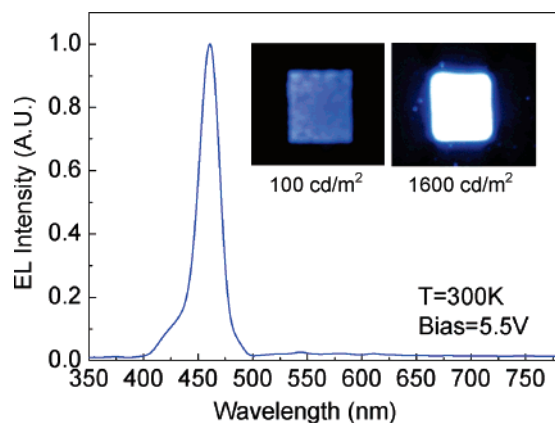


Figure 3. Electroluminescence spectrum of the QD-LED measured at the bias of 5.5 V. Insets: photomicrographs of the LED surface recorded at the brightnesses of 100 and 1600 cd/m^2 .

reduction of quantum yield of QDs as a consequence of the loss of surface passivation when the amount of surfactant molecules over the nanocrystal drops rapidly in the purification process. In our experiment, the purified QD power appeared stable for shelf storage, as shown in Inset I of Figure 1a, and retains a high quantum yield $\sim 25\%$ in toluene solution.

Noteworthy is that there are no noticeable deep trap emissions over the entire visible range of the room-temperature PL spectra for both CdS core and CdS/ZnS core/shell QDs. This is in sharp contrast to early reports where a significant portion of (or the whole emission of) CdS cores were due to deep trap centers and only became suppressed upon the growth of ZnS shells.^{15,18} The device quality of the QD material prepared for our blue-LED processing is further confirmed by the high-resolution transmission electron microscopic (HR-TEM) image of the nanocrystals, as shown in Inset II of Figure 1a. In the TEM picture, the core-shell QD exhibits an approximately spherical shape with a diameter near 4 nm. The well-resolved regular lattice fringes

indicate the single crystalline nature of the core/shell structures without detectable stacking faults and other defects.

A multilayer structure of ITO/poly(3,4-ethylenedioxythiophene) poly(styrenesulfonate) (PEDOT/PSS) (25 nm)/hole transport layer (HTL) (45 nm)/QDs (~ 3 MLs)/Al (150 nm) was employed in the fabrication of the blue QD-LEDs, with stripe-patterned ITO/PEDOT/PSS as the anode, poly(*N,N'*-bis(4-butylphenyl)-*N,N'*-bis(phenyl)benzidine) (poly-TPD) spin-coated from chlorobenzene solution as the HTL, QD layer spin-coated from a toluene solution as the emissive layer, and shadow-mask-evaporated Al lines as the cathode. The fabricated QD-LED devices, each with a surface area of 4 mm^2 , were defined by the intersection of the orthogonally aligned stripes of ITO and Al electrodes. The energy level diagram of the device was plotted in Inset III of Figure 1b. The highest occupied molecular orbit level of Poly-TPD is ~ 5.2 eV, close to the work function of the ITO/PEDOT anode, which facilitates the hole transport from the anode to the emissive QD layer. The conduction band-edge of the CdS/ZnS QDs was determined from the measured optical band gap in combination with an effective mass approximation calculation.²¹ There is no barrier for electron injection between the Al cathode and the emissive QDs.

In the earlier reported fabrication of blue QD-LEDs, QDs were blended with HTL molecules such as 4,4'-*N,N'*-dicarbazolyl-biphenyl and *N,N'*-diphenyl-*N,N'*-bis(3-methylphenyl)-(1,1 0-biphenyl)-4,4 0-diamine (TPD) prior to the spin-cast deposition of device-active regions.^{13,15,16,17} Consequently, each emissive QD was partially or completely surrounded by organic molecules allowing for the direct energy transfer from organic molecules to QDs for enhanced LED quantum efficiencies. Because there were excitons created in the organic molecules, however, the incomplete energy transfer often led to the broad organic emission that deteriorates the color purity of blue QD-LEDs. In the present device processing the deposition of the HTL layer is separated from that of the QD layer resulting in a poly-TPD/QD bilayer structure. When the QD thickness is optimized

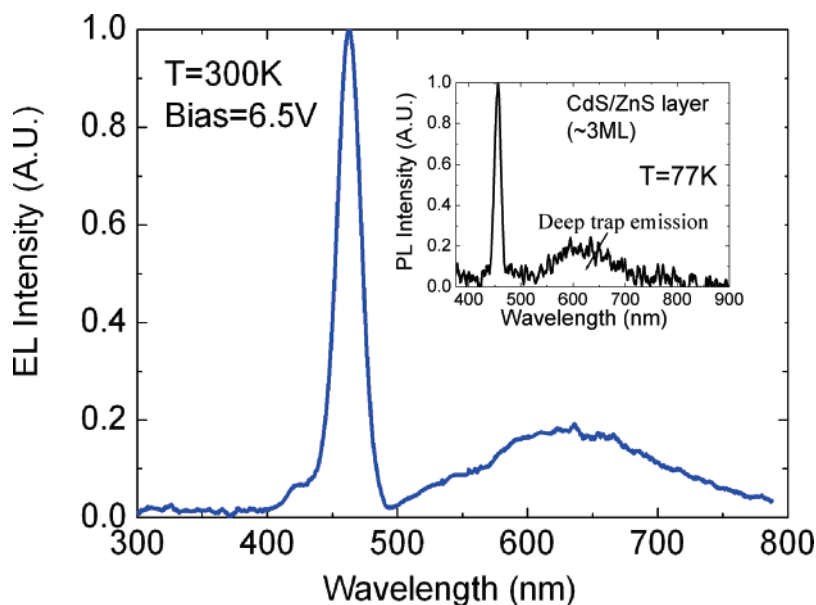


Figure 4. Electroluminescence spectrum of the QD-LED measured at the bias of 6.5 V. Inset: photoluminescence spectrum of CdS/ZnS QDs in the LED active region measured at 77 K.

(equivalent to ~ 3 MLs), radiative recombination of electrons and holes can be largely confined in the QD region for a more saturated blue emission of QD-LEDs. Poly-TPD exhibits an intrinsic resistance to nonpolar organic solvents such as toluene and xylene, allowing the solution casting of QD films over poly-TPD surfaces. In addition, the luminescence efficiency of poly-TPD is substantially lower than that of the QDs, which helps to minimize the residual organic emission in the LED output. The similar strategy has been applied in the early development of red QD-LEDs for organic-free emission.²² The exclusion of an Alq3 electron transport layer in the device configuration serves the same purpose.

The current–voltage characteristics of QD-LEDs were measured with a Keithley 4200 semiconductor parameter analyzer. An Ocean Optic UV–vis–NIR spectrophotometer was used to study the LED output spectra. To determine the photometric brightness (cd/m^2) of the QD-LED, the diode output power was first measured with a Newport 1830-C power meter and a Newport 818SL silicon photodetector that was directed at a fixed distance toward the ITO glass side of the QD-LED. The LED luminance (brightness) and luminous efficiency was then calculated from the known portion of the forward emission and the LED output spectra. Images of LED output were recorded with a Sony DFW-X700 FireWire color charge-coupled device camera coupled with a C-mount lens. All the measurements were performed under ambient conditions.

Figure 2 plots the measured current density and luminance of the QD-LED as functions of the applied voltage (I – V and P – V). The onset voltage, which is defined as the bias voltage applied to an LED producing a brightness of $0.1 \text{ cd}/\text{m}^2$, is as low as 2.5 V. The LED luminance reaches $1600 \text{ cd}/\text{m}^2$ at a bias of 5.5 V. The low-operating voltage and the high brightness achieved in our blue QD-LEDs became comparable to that of red and green QD devices, closing

the performance gap between blue and red/green QD-LEDs. The inset of Figure 2 shows the luminance efficiency versus injection density. A maximum luminance efficiency of $0.506 \text{ cd}/\text{A}$ was achieved at $I = 70.8 \text{ mA}/\text{cm}^2$, corresponding to the LED brightness of $351 \text{ cd}/\text{m}^2$. While the measured efficiency appears lower than the value reported by Jun et al.,¹⁶ it is associated with a narrow band blue emission that is featured by a small luminous efficacy of ~ 0.06 as compared to the large efficacy (~ 0.95) of the high-intensity green tail presented in the emission of Jun's blue-LEDs.

Figure 3 shows the EL spectrum of the device at the brightness of $1600 \text{ cd}/\text{m}^2$. The LED emission peaks at 460 nm with the measured fwhm bandwidth is as narrow as 20 nm. The spectral characteristic of the LED output resembles that of the PL emission of the QD solution except for a small shoulder in the UV region due to the residual emission from the poly-TPD ($\lambda_{\text{peak}} \sim 410 \text{ nm}$). There is no noticeable shift of the peak wavelength between the EL and PL emission. The integrated intensity of the broad, long-wavelength tail over the green and red spectral regions has been reduced to less than 5% of the total emission of the device, ensuring the spectral purity of blue light output from the QD-LED.

It is worth mentioning that the narrow bandwidth ($\sim 20 \text{ nm}$) of the blue QD-LEDs reported herein is comparable to that of epitaxially grown, single-crystal III–V compound devices,²³ such as (Al,Ga)N blue LEDs, reflective of the inherently inorganic, crystalline nature of CdS/ZnS QDs used as the emissive elements of our LED device. This compares favorably to the organic LEDs, the emission of which is often featured with a large bandwidth ($\geq 60 \text{ nm}$). The inset shows the photomicrographs of the LED surface taken at 100 and $1600 \text{ cd}/\text{m}^2$, respectively. At high brightness, the LED image becomes whitish due to the saturation of the camera sensor pixels, while the periphery region glows blue as a result of the back scattering.

When the voltage applied to the LED device was increased beyond 5.5 V, there was a distinct rise of a broad peak in the long-wavelength regime. The integrated intensity of the broad peak became ~50% of the total LED emission at the bias of 6.5 V, as shown in Figure 4. It is speculated that this long-wavelength signal arises from the deep-level emission from the quantum dots as a consequence of irreversible defect formation under high current-injection ($\sim 0.6 \text{ A/cm}^2$ at 6.5 V-bias).^{18,24} This was verified by the low-temperature PL study of the emissive QDs in the device active region, as shown in the inset of Figure 4. At 77 K, other than the strong band-edge PL emission, a broadband PL signal of a deep transition was identified, centered at $\sim 610 \text{ nm}$, which matches well with the long-wavelength peak of the EL emission under high bias. A further study on the high current-induced deep-level emission from QDs is currently underway.

Acknowledgment. The work at the Penn State University is being supported by the National Science Foundation under Grant CMMI-0729263 and Army Research Office under Grants DAAD19-02-D-0001, and that at Ocean NanoTech LLC. is supported by the National Science Foundation under Grant 0638209. Q.Z. and S.E.M. are grateful to the NSF NNIN through Grant 0335765 for operation of the TEM facility and ARO W911NF0510334 for partial financial support.

References

- Colvin, V. L.; Schlamp, M. C.; Alivisatos, A. P. Light Emitting Diodes Made from Cadmium Selenide Nanocrystals and a Semiconducting Polymer. *Nature* **1994**, *370*, 354.
- Dabbousi, B. O.; Bawendi, M. G.; Onitsuka, O.; Rubner, M. F. Electroluminescence from CdSe quantum-dot/polymer composites. *Appl. Phys. Lett.* **1995**, *66*, 1316–1318.
- Kumar, N. D.; Joshi, P. M.; Friend, C. S.; Prasad, P. N.; Burzynski, R. Organic–inorganic heterojunction light emitting diodes based on poly(p-phenylene vinylene)/cadmium sulfide thin films. *Appl. Phys. Lett.* **1997**, *71* (10), 1388–1390.
- Schlamp, M. C.; Peng, X.; Alivisatos, A. P. Improved efficiencies in light emitting diodes made with CdSe/CdS core/shell type nanocrystals and a semiconducting polymer. *J. Appl. Phys.* **1997**, *82* (11).
- Gao, M.; Lesser, C.; Kirstein, S.; Mohwald, H.; Rogach, A. L.; Weller, H. Electroluminescence of different colors from polycation/CdTe nanocrystal self-assembled films. *J. Appl. Phys.* **2000**, *87*, 2297–2302.
- Coe, S.; Woo, W.-K.; Bawendi, M.; Bulovic, V. Electroluminescence from single monolayers of nanocrystals in molecular organic devices. *Nature* **2002**, *420*, 800–803.
- Yang, H.; Holloway, P. H.; Ratna, B. B. Photoluminescent and electroluminescent properties of Mn-doped ZnS nanocrystals. *J. Appl. Phys.* **2003**, *93*, 568–592.
- Chaudhary, S.; Ozkan, M.; Chan, W. C. W. Trilayer hybrid polymer-quantum dot light-emitting diodes. *Appl. Phys. Lett.* **2004**, *84*, 2925–2927.
- Steckel, J. S.; Snee, P.; Coe-Sullivan, S.; Zimmer, J. P.; Halpert, J. E.; Anikeeva, P.; Kim, L.-A.; Bulovic, V.; Bawendi, M. G. Color-Saturated Green-Emitting QD-LEDs. *Angew. Chem., Int. Ed.* **2006**, *45*, 5796–5799.
- Xu, J.; Cui, D.; Gerhold, M.; Wang, A. Y. Microcavity Light Emitting Devices Based on Colloidal Semiconductor Nanocrystal Quantum Dots. *IEEE Photon. Technol. Lett.* **2005**, *17*, 2008–2010.
- Coe-Sullivan, S.; Steckel, J. S.; Kima, L.; Bawendi, M. G.; Bulovic, V. Method for fabrication of saturated RGB quantum dot light emitting devices. *Proc. SPIE* **2006**, *5739*, 108–115.
- Moeller, G.; Coe-Sullivan, S. Quantum-Dot Light-Emitting Devices for Displays. *Information Display* **2006**, *2/06*, 2–6.
- Rizzo, A.; Li, Y.; Kudera, S.; Della Sala, F.; Zanella, M.; Parak, W. J.; Cingolani, R.; Manna, L.; Gigli, G. Blue light emitting diodes based on fluorescent CdSe/ZnS nanocrystals. *Appl. Phys. Lett.* **2007**, *90*, 051106.
- Widdel, H.; Post, D. L. *Color in Electronic Displays*, 1st ed.; Springer: New York, 1992.
- Steckel, J. S.; Zimmer, J. P.; Coe-Sullivan, S.; Stott, N. E.; Bulović, V.; Bawendi, M. G. Blue Luminescence from (CdS)/ZnS Core–Shell Nanocrystals. *Angew. Chem., Int. Ed.* **2004**, *43*, 2154–2158.
- Jun, S.; Jang, E. Interfused semiconductor nanocrystals: brilliant blue photoluminescence and electroluminescence. *Chem. Commun.* **2005**, 4616–4618.
- Anikeeva, P. O.; Halpert, J. E.; Bawendi, M. G.; Bulovic, V. Electroluminescence from a Mixed Red-Green-Blue Colloidal Quantum Dot Monolayer. *Nano Lett.* **2007**, *7* (8), 2196–2200. Note: In Figure 2 of this reference, the blue EL emission from ZnCdS alloyed quantum dots appears to have narrow bandwidth along with a long spectral tail covering green and red wavelengths. There is no explicit information in the context on the bandwidth of the reported blue emission.
- Protière, M.; Reiss, P. Facile synthesis of monodisperse ZnS capped CdS nanocrystals exhibiting efficient blue emission. *Nanoscale Res. Lett.* **2006**, *1*, 62–67.
- Li, J. J.; Wang, Y. A.; Guo, W.; Keay, J. C.; Mishima, T. D.; Johnson, M. B.; Peng, X. Large-scale synthesis of nearly monodisperse CdSe/CdS core/shell nanocrystals using air-stable reagents via successive ion layer adsorption and reaction. *J. Am. Chem. Soc.* **2003**, *125*, 12567–12575.
- Sun, Q.; Wang, Y. A.; Li, L. S.; Wang, D.; Zhu, T.; Xu, J.; Yang, C.; Li, Y. Bright and Color-Saturated Red, Orange, Yellow and Green Light Emitting Diodes Based on Core/Shell Quantum Dots with CdSe Cores. *Nature Nanophotonics*, submitted for publication.
- Xia, J. Electronic Structures of Zero-Dimension Quantum Wells. *Phys. Rev., B* **40**, 8500–8507.
- Bardecker, J. A.; Munro, A. M.; Liu, M. S.; Niu, Y.; Ding, I.-K.; Luo, J.; Chen, B.; Jen, A. K.-Y.; Ginger, D. S. Efficient CdSe/CdS quantum dot light-emitting diodes using a thermally polymerized hole transport layer. *Nano Lett.* **2006**, *6*, 463–467.
- Zhang, B.; Liang, H.; Wang, Y.; Feng, Z.; Ng, K. W.; Lau, K. M. “High-performance III-nitride blue LEDs grown and fabricated on patterned Si substrates. *J. Cryst. Growth* **2007**, *298*, 725–730.
- Katona, T. M.; Margalith, T.; Moe, C.; Schmidt, M. C.; Nakamura, S.; Speck, J. S.; DenBaars, S. P. Growth and Fabrication of Short Wavelength UV LEDs. *Proc. SPIE* **2004**, *5187*, 250–259.

NL072370S